Eur. Phys. J. A (2016) **52**: 80
DOI 10.1140/epja/i2016-16080-7

THE EUROPEAN PHYSICAL JOURNAL A

Review

Calibration of the solar neutrino detectors*

Barbara Caccianiga[a] and Alessandra Carlotta Re

Università degli Studi and INFN, Sezione di Milano, Via Celoria 16, 20133 Milano, Italy

Received: 7 July 2015
Published online: 8 April 2016 –
Communicated by C. Broggini

Abstract. Calibrations have been crucial for the success of solar neutrino experiments. In this contribution we review the calibration strategies adopted by different solar neutrino experiments. In particular, we will emphasize their common critical aspects and their main differences. In order to do so, we will schematically divide the solar neutrino experiments in two groups: those based on radiochemical techniques, *i.e.* Homestake, Gallex/GNO, SAGE and those based on real-time techniques *i.e.* Kamiokande, Super-Kamiokande, SNO, Borexino and KamLAND.

1 Introduction

The solar neutrino experimental era was started nearly 50 years ago by the pioneering work of the radiochemical experiment Homestake. This ground-breaking effort was followed and complemented by several other experiments based on different techniques: Gallex/GNO, SAGE (radiochemical), Kamiokande, Super-Kamiokande, SNO (water Cherenkov) KamLAND and Borexino (liquid scintillator) (see [1, 2] and [3] for details). The combined results of all the solar neutrino experiments has provided a coherent and complete picture which on one side confirms the Standard Solar Model (see [4]) and on the other evidentiates the neutrino oscillation phenomenon, allowing to determine the oscillation parameters Δm^2_{12} and θ_{12} (see [5]). Calibrations have played a key role in this successful enterprise: at the beginning, by giving confidence in the somehow surprising results coming from the first-generation experiments (which gave birth to the so-called "solar neutrino problem"); later on, by providing the second-generation experiments with the strict control on systematics needed for precision measurements. This article is devoted to a critical discussion of the calibration strategies adopted by different solar neutrino experiments: in particular, we will stress common issues and main differences between them. For the sake of brevity, we will not discuss low-level electronics calibrations (such as timing or charge equalization procedures). We will instead focus the attention on the methods adopted to validate and characterize the most important elements contributing to the analysis of each specific experiment, such as, for example, the detection efficiency, the energy scale, the position reconstruction capability.

Neutrinos are elusive particles which are difficult to detect because of their low interaction probability. To overcome this problem, all solar neutrino experiments adopt large target masses, combined with high detection sensitivity, low background environment and deep underground location in order to maximize the signal, while reducing both internal and external backgrounds. We can schematically divide the solar neutrino experiments in two cathegories: those based on radiochemical techniques (Homestake, Gallex and SAGE) and those based on real-time techniques (Kamiokande, Super-Kamiokande, SNO, KamLAND, and Borexino). The former measure the neutrino flux by counting the number of nuclei produced by the interacting neutrinos in a large amount of target material. For this class of experiments, calibrations have been essential to verify that the complete detection chain (production and collection of the daughter nuclei) is fully efficient. We will discuss the calibration strategy for this class of detectors in sect. 2.

In real-time experiments the detection efficiency is not expected to contribute significantly to the global uncertainty of the measurement (except for few special cases which will be mentioned in the following). On the other hand, real-time experiments rely critically on the signal to noise separation provided by several observables (position, energy, time) which must be determined precisely on an event-by-event basis. For this class of experiments, therefore, calibrations have been crucial to precisely assess the energy scale, the performance of the position reconstruction alghoritm and so on. We will discuss the calibration strategy for real-time experiments in sect. 3.

* Contribution to the Topical Issue "Underground nuclear astrophysics, and solar neutrinos: Impact on astrophysics, solar and neutrino physics" edited by Gianpaolo Bellini, Carlo Broggini, Alessandra Guglielmetti.

[a] e-mail: barbara.caccianiga@mi.infn.it

2 The radiochemical experiments

The radiochemical technique is based on the principle that neutrinos can induce reactions which transform a specific target nucleus into a different one. The daughter nuclei produced by the neutrino interactions can be chemically separated from the target mass and counted through low background proportional counters. This technique is sensitive to the total capture rate above a certain threshold (depending on the chosen isotope) but does not convey any information on the neutrino exact timing and energy spectrum.

2.1 The Homestake experiment

The Homestake detector consisted of about 615 tons of C_2Cl_4 where solar electron neutrinos were revealed via the reaction

$$^{37}\mathrm{Cl} + \nu_\mathrm{e} \rightarrow {}^{37}\mathrm{Ar} + \mathrm{e}^-,$$

with an energy threshold of 0.814 MeV. The solar neutrino flux measurement critically depends on the production, extraction and counting of the argon nuclei. In this context, calibrations consist in a number of experimental checks specifically carried out to ensure that the efficiency of each step and of the overall detection procedure is under control. The argon recovery is a crucial point: it requires the efficient extraction of small quantities of Ar (fractions of a cubic centimeter) produced by neutrinos in the large C_2Cl_4 volume. This is obtained by purging the liquid with large amount of Helium gas. The recovery efficiency for the ^{37}Ar present in the tank is determined routinely by inserting a measured amount of isotopically separated argon gas (^{36}Ar or ^{38}Ar) in the tank at the beginning of each exposure. The extraction efficiency is the ratio of the amount of isotopically labeled carrier gas that is recovered in the extraction process to the amount of that carrier gas inserted into the tank. The validity of this method depends on the absence of chemical traps which would affect only the internally produced argon. In fact, ^{37}Ar produced in the neutrino interaction could remain bound to the remnants of the C_2Cl_4 molecule thus reducing its collection efficiency. This possibility was tested in a separate apparatus which used C_2Cl_4, with ^{36}Cl atoms. ^{36}Cl is unstable with a half life of 3×10^5 years and beta decays into ^{36}Ar. Since the energy spectrum of ^{36}Ar in these decays is similar to that of ^{37}Ar produced by solar neutrino interactions, full recovery of the ^{36}Ar from the ^{36}Cl labeled C_2Cl_4 would imply that argon atoms are not trapped in the remnant molecule. After an appropriate time period the ^{36}Ar was swept out of the labeled C_2Cl_4. The recovery of ^{36}Ar was 1.02 ± 0.039 of that predicted from the ^{36}Cl life time indicating that molecular trapping did not occur.

After extraction, argon is purified and inserted in proportional counters to determine its production rate. The determination of the efficiency of this particular step of the detection chain is performed separately by filling each counter with a calibrated amount of ^{37}Ar, obtained by irradiating ^{40}Ca with neutrons. The absolute ^{37}Ar activity is measured in large counters (internal volume of 100 cm^3 with an active region 30 cm long by 2 cm diameter) that are especially made for this purpose.

A test of the overall detection efficiency (argon extraction + counting) was performed by means of a radium-beryllium neutron source inserted in a re-entrant iron pipe that reaches to the center of the tank. The liquid was irradiated with this source producing ^{37}Ar via the chain of reactions $^{35}\mathrm{Cl}(\mathrm{n},\mathrm{p})^{35}\mathrm{Sr}$ followed by $^{37}\mathrm{Cl}(\mathrm{p},\mathrm{n})^{37}\mathrm{Ar}$. The total ^{37}Ar production rate measured by extracting and counting the argon nuclei with the standard detection chain is in agreement with what expected, thus proving that the efficiency for detecting neutrinos is under control. The overall contribution of extraction and counting efficiencies to the systematic error on the solar neutrino rate has been evaluated on the basis of the tests decribed above to be 6.1% [6].

2.2 The Gallex/GNO and SAGE experiments

The Gallex (GALLium EXperiment) and the SAGE (Soviet-American Gallium Experiment) have used ^{71}Ga as target for the reaction:

$$^{71}\mathrm{Ga} + \nu_\mathrm{e} \rightarrow {}^{71}\mathrm{Ge} + \mathrm{e}^-.$$

The choice of isotope ^{71}Ga as target was due to its very low-energy threshold (0.233 MeV) which makes it possible to detect the most abundant class of solar neutrinos: the pp neutrinos.

The SAGE detector consisted of 30 tons (later increased to 57 tons) of liquid metallic gallium. Gallex consisted of 30 tons of $GaCl_3$-HCl. Once the Gallex program was completed, its direct successor, the GNO experiment (Gallium Neutrino Observatory), took data for about 5 more years.

The Gallex/GNO calibration

Gallex is a very difficult experiment aiming at the detection of just few atoms in a large volume of gallium chloride target solution. As for the other radiochemical experiments the credibility of its results must be demostrated by convincing tests concerning the full detection chain which includes production, recovery and counting of ^{71}Ge atoms. Two main types of calibrations were performed during Gallex/GNO data-taking: calibrations with a ^{51}Cr neutrino source which validates the entire detection procedure (including the neutrino capture mechanism) and several tests with ^{71}As which are focused on the ^{71}Ge extraction efficiency.

Gallex performed two calibration campaigns with a very intense ^{51}Cr neutrino source (> 60 PBq). ^{51}Cr decays by electron capture to ^{51}V with a half-life of 27.7 days, emitting two monocromatic neutrino lines at 750 keV and 430 keV respectively. Two ^{51}Cr calibration runs have been performed: each time, the same source of about 36 kg in form of small irregular chips (≈ 1 mm^3) was irradiated in

the french Siloé reactor, placed in a sealed tungsten shield, and then shipped to the Laboratori Nazionali del Gran Sasso. Since the nominal source activity was the analysis key-point, several independent methods were used to determine it: ^{51}Cr samples were evaluated in an ionization chamber, via gamma spectroscopy, via calorimetry and by studying the quantity of ^{51}Cr stable daughter, the ^{51}V. The source remained in the center of the experiment for about 4 months. The ratio of measured to nominal source activity obtained combining the two ^{51}Cr calibration data was found to be 0.93 ± 0.08 [7]. This result excludes large systematic errors in each step of the detection chain, in particular those concerning the uncertainty on the cross-section of the neutrino capture reaction.

For what concerns the collection and recovery efficiency of ^{71}Ge, simple labeling with inactive germanium spikes was routinely done with milligram carriers in every run for yield monitoring. However, this is not sufficient to rule out possible non trivial chemical behaviour of the ^{71}Ge atoms produced by the neutrino interactions. In order to take these effects into account, systematic studies were performed by adding a known amount of ^{71}As to the target solution. This isotope beta decays to ^{71}Ge (half-life = 2.72 days), with recoil energies that are similar to the one involved in the neutrino-induced production of ^{71}Ge. The ^{71}As nominal activity was precisely determined via Ge(HP) spectroscopy at the Gran Sasso underground facility. The test with ^{71}As was not possible during regular solar neutrino recording phases, since it implied to severely contaminate the detector. It was possible only during prolongued maintenance periods like for example, between the end of Gallex solar observations and the start of GNO. Several tests with ^{71}As were performed and showed a substantial agreement between the rate of ^{71}Ge rate (measured following the same procedure of the standard solar runs) and the predictions coming from the precisely known nominal ^{71}As activity. In conclusions, the ^{51}Cr source and the ^{71}As tests have validated the Gallex detection procedure, ruling out the possibility that the observed solar neutrino deficit is due to an experimental artefact [8].

The SAGE calibration

The calibration strategy of SAGE is similar to the one adopted by other radiochemical experiments.

The insertion of small amounts of stable Ge at the beginning of each solar neutrino run is used to routinely verify the extraction efficiency, which is typically found to be in the range of (80–90)%. The systematic uncertainty in this efficiency is 3.4%, mainly arising from uncertainties in the mass of added and extracted carrier.

Two neutrino sources were used in SAGE to validate the entire detection procedure at different energies: an artificial ^{51}Cr neutrino source (two monocromatic neutrino lines at 750 keV and 430 keV) and a ^{37}Ar neutrino source (monocromatic neutrino line at 811 keV). The ^{51}Cr activity was about 19 PBq and was measured via different approaches: calorimetry, direct counting (via gamma spectroscopy) and reactor physics. The overall uncertainty on the source activity was about 5%. The source was placed at the center of a 13 tons target of liquid gallium (in a specifically dedicated apparatus separate from the main detector) and, using the same procedure as for solar neutrino measurements, the ^{71}Ge atoms extracted from the target were measured in proportional chambers. The ratio between measured and expected ^{71}Ge rates was found to be 0.95 ± 0.12 [9].

The SAGE collaboration performed also another test with a ^{37}Ar neutrino source in order to study the neutrino capture rate at energies close to the solar ^{7}Be neutrino line. The source was produced via the reaction $^{40}\mathrm{Ca}(\mathrm{n},\alpha)^{37}\mathrm{Ar}$. The ^{37}Ar nominal activity was measured using three different methods: mass spectrometry (two measurements at the fabricating reactor, one at the source production, the other after the exposure), calorimetry at the detector site, and via proportional counters once back at the fabricating reactor. The ratio of measured to nominal source activity obtained with the ^{37}Ar calibration data was found to be $0.79^{+0.09}_{-0.10}$ [10].

The results from the ^{51}Cr and ^{37}Ar source calibrations provided a strong verification of the experimental efficiencies [10] and validated the fundamental assumption in radiochemical experiments that the extraction efficiency of atoms produced by neutrino interactions is the same as that of the stable carrier.

3 Calibrations in real-time experiments

Real-time experiments exploit the Cherenkov or scintillation technique to detect solar neutrinos. Unlike radiochemical experiments which simply count the number of neutrino induced interactions in the detector, real-time experiments collect many information concerning each neutrino induced event: time, energy, position, possibly direction (in case of Cherenkov detectors). The energy is proportional to the number of collected (Cherenkov or scintillation) photons, while event position and direction can be determined from the time and space pattern of the hit phototubes. This pattern critically depends on the characteristics of the photon-emission process and on the optical properties of the detector. In fact, given the typically large dimensions of solar neutrino experiments, absorption, scattering and other processes can perturb significantly the photon propagation from the production to the detection point.

For these reasons, in order to be able to reconstruct physical quantities with a small systematic uncertainty, real-time experiments require to know in detail the detector response throughout the entire active volume. Calibrations play a decisive role to achieve this goal, in combination with detailed Monte Carlo simulations. The general calibration strategy adopted by all experiments is based on sources emitting different types of particles (α, β, γ, neutrons), deployed throughout the detector volume in order to precisely determine the energy scale, the uniformity of the response and the position/direction reconstruction capability. Sources are selected in order to cover

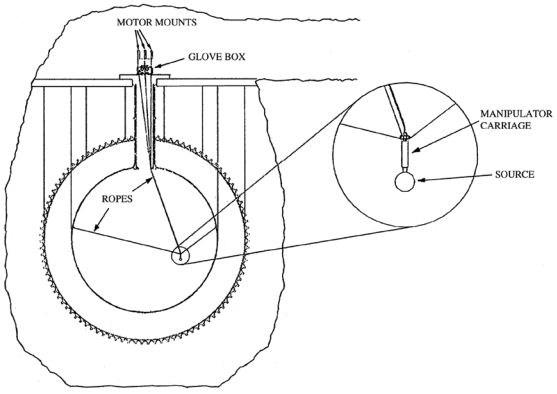

Fig. 1. SNO: source insertion system.

the energy range of interest for the specific experiment: above ~ 3 MeV for Super-Kamiokande and SNO, down to ~ 100 keV for Borexino. In addition, light sources are used to study the detector optical properties (transparency, scattering ...), which are then used as input for Monte Carlo simulations. In the following paragraphs we will describe the details of the calibrations performed specifically by each real-time experiment, SNO, Super-Kamiokande, Borexino and KamLAND.

3.1 Calibrations in SNO

The Subdury Neutrino Observatory (SNO) employs 1000 tons of heavy water to detect neutrinos via three different reactions:

$$\nu_e + d \rightarrow p + p + e^- \quad \text{(Charged Current reaction)}$$
$$\nu_x + e^- \rightarrow \nu_x + e^- \quad \text{(Elastic Scattering reaction)}$$
$$\nu_x + d \rightarrow p + n + \nu_x \quad \text{(Neutral Current reaction).}$$

Charged current and scattering reactions are tagged by detecting the outcoming electron via the Cherenkov light it emits. Neutral current reactions are tagged by detecting the outcoming neutron. This is done in three different ways corresponding to three Phases of the experiment: in Phase 1 (1999–2001), neutrons are detected by capture on deuteron (which is followed by the emission of a 6.25 MeV γ); in Phase 2 (2001–2003), neutrons are detected by capture on ^{37}Cl (which is followed by the emission of multiple γ's with a total energy of 8.6 MeV); in Phase 3 (2003–2006), neutrons are detected by an array of ^{3}He proportional counters (NCD).

Calibrations in SNO have been extensively performed during all three Phases, employing different types of sources: point-like radioactive sources, point-like optical sources, uniformly distributed radioactive-sources.

Point-like sources have been deployed within the SNO D_2O volume by means of a general purpose manipulator (see fig. 1), which allows to reach multiple positions on the XZ and YZ planes covering 70% of each plane. The position accuracy is better than 5 cm. The system is equipped with a glove box that is part of the cover-gas volume and allows to work on a source while keeping the detector isolated from light and airborne radioactivity.

Energy scale, position and direction reconstruction

The main radioactive sources used in SNO for this purpose are ^{16}N and ^{8}Li. They are both produced *in situ* in a utility room near the SNO cavity, by means of a commercially available Deuterium-Tritium (DT) fast neutron generator. The ^{16}N isotope is produced via the (n, p) reaction on ^{16}O and transferred to the water volumes in a CO_2 gas stream via small diameter capillary tubing. It decays beta-gamma with an half-life of 7.13 s and with a Q-value of 10.4 MeV. The source is contained in a chamber designed to block the β particles allowing the 6.13 MeV γ's to exit. The blocked β particles are detected by a plastic scintillator lining of the chamber, providing a trigger for the SNO electronics [11]. The ^{8}Li isotope is created via the (n, α) reaction on ^{11}B and is carried to a decay chamber using a gas/aerosol transport system. It decays β (Q-value = 16 MeV) producing a spectrum in the same energy range as the ^{8}B solar neutrinos (the main goal for SNO). The β signal is promptly followed by the emission of alpha-particles which are used to tag the event. Note that, in order to obtain a precise energy calibration from this source, it is important to carefully account for energy losses in the walls of the decay chamber [12]. In Phase I the linearity of the energy scale was also tested using a proton-triton fusion (pT) source, which produces gamma-rays of 19.8 MeV. Gammas are emitted in the ^{3}He(p, γ)^{4}He reaction by ~ 30 keV protons impinging on a high-purity scandium tritide target. The total length of the pT source (including the proton generator and accelerator and the target) is only 50 cm. For deployment in SNO, it was housed inside a 25.4 cm diameter by 60 cm long stainless-steel cylindrical deployment capsule [13].

Response to neutrons

Two point-like sources were used to measure the neutron detection efficiency and its uniformity throughout the active volume: ^{252}Cf and ^{241}Am^{9}Be. As an example, fig. 2 shows the results of the calibrations performed with the ^{252}Cf source (activity = 16 n/s) in Phase 1 (capture of neutron on pure heavy water) and Phase 2 (capture of neutron on ^{37}Cl after the addition of NaCl). In addition to these point-like neutron sources, a uniformly distributed ^{24}Na source was used to study the neutron detection efficiency and to characterize the NCD neutron response [14]. This calibration was performed by injecting in the D_2O volume a small amount of heavy water loaded with ^{24}Na. ^{24}Na, which decays β-γ with a Q-value = 5.516 MeV, produces neutrons through deuteron photodisintegration. Its lifetime (half-life = 14.93 hours) is long enough to guarantee time for mixing, while avoiding permanent contamination of the detector. This calibration method turned out to be especially important in Phase 3 when the NCD array was deployed: in fact the discrete locations of the NCD

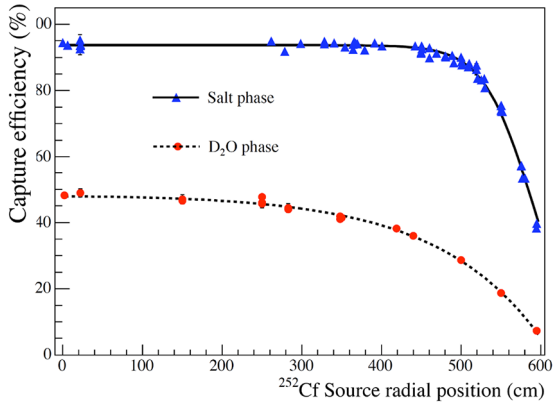

Fig. 2. SNO: neutron detection efficiency as a function of position measured with a ^{252}Cf source in SNO Phase 1 and Phase 2.

detectors made the uncertainties related to the point-like source position much more significant. Besides neutron efficiency study, the decay of ^{24}Na provided also a calibration of the SNO response to low energy β's and γ's.

Study of radioactivity-induced background

In SNO, the background Cherenkov light below 4.5 MeV is predominantly due to trace amount of natural radioactivity, in particular from the ^{238}U e ^{232}Th chain. If the γ's emitted in the radioactive decays are above the deuteron binding energy, they can produce neutrons by photodisintegration, which are indistinguishable from neutrons produced in the neutrino induced neutral current events. A number of controlled spikes of ^{222}Rn were made in the SNO detector in order to test the Monte Carlo description of the detector response to radon and its daughters (in particular ^{214}Bi) and of the yield of neutrons produced through deuteron photodisintegration.

Calibrations with optical sources

The optical properties of the SNO heavy water are measured in situ using a spherical light diffuser [15]. Light from a pulsed nitrogen/dye laser is conveyed to the diffuser by means of specially developed underwater optical fiber umbilical cables. The laserball can be moved to many positions in the D_2O and H_2O volumes. Six different laser wavelenghts (ranging from 337 nm to 619 nm) are used. Data collected with this source are employed to determine the absorption and scattering of light in the heavy water and light water, and the angular dependence of the response of the detector's photomultiplier tubes.

A summary of the sources used for calibration by the SNO experiment can be found in table 1.

3.2 Calibrations in Super-Kamiokande

Super-Kamiokande is a large water Cherenkov detector consisting of 50 ktons of water. It detects solar neutrinos via the scattering reaction

$$\nu_x + e^- \rightarrow \nu_x + e^-.$$

The Cherenkov technique allows to reconstruct both energy and direction of the outcoming electrons. The analysis of solar neutrino requires to know precisely the absolute energy scale, energy resolution, angular resolution, spatial resolution and detection efficiency for low-energy (few MeV) electrons. These information are provided by calibrations which are performed regularly during data taking. In the following we will summarize the most important ingredients of the Super-Kamiokande calibration strategy which have been important throughout all Phases of the long experiment life.

Energy, position and direction reconstruction

Super-Kamiokande uses two sources of electrons: an electron linear accelerator (LINAC) and a ^{16}N source (see [18], [19] and [20] for more details). A scheme of the LINAC system is shown in fig. 3. The LINAC accelerator is located in a tunnel aside of the Super-Kamiokande detector and produces electrons of well-controlled energy. The beam is bended by a system of magnets (D1, D2, D3) and is injected in a vertical pipe of variable lenght which can be deployed in nine different positions of the detector volume. The endcap of the beam pipe is closed by a 100 μm thick titanium window of 3 cm diameter which guarantees minimal energy loss and multiple scattering for electrons down to 5 MeV. The LINAC calibration data are crucial to tune the MonteCarlo which is then used to extrapolate the detector energy response in all positions and all directions throughout the water volume. The overall uncertainty on the absolute energy scale between 5 and 16.3 MeV obtained with this method is better than 1%. The LINAC calibration is also used to study the direction and position reconstruction.

The energy calibration is also performed with a ^{16}N source. In particular, since events from ^{16}N decay are isotropic, they are useful in probing the directional dependence of the energy scale. ^{16}N predominantly decays by emitting an electron (maximum energy 4.3 MeV) in coincidence with a 6.1 MeV gamma ray. ^{16}N is produced by the interaction of fast neutrons from a Deuterium-Tritium generator (DTG) on the ^{16}O nuclei of the detector water. This *in situ* production is obtained by deploying the DTG in the detector. After firing, the DTG is withdrawn, leaving the produced ^{16}N to decay unaffected by the presence of any calibration equipment (see fig. 4).

A Ni-Cf source is also used in Super-Kamiokande's calibrations. This source emits γ's by thermal neutron capture on nickel through the reaction Ni(n, γ)Ni. Neutrons are produced by the spontaneous fission of ^{252}Cf. Given the complex geometry of this source and the complicated nuclear de-exitation process, the energy spectrum of the emitted γ's is affected by large systematic errors. For this reason, the Ni-Cf source is not used in absolute energy calibrations. On the other hand it is essential for systematic studies on vertex reconstruction capability.

Table 1. SNO: summary of the calibration source.

Source	Type	E [MeV]	Position	Motivations
^{16}N	γ	6.1	multiple positions in D_2O	Energy scale, detector response
^{8}Li	β	< 16	multiple positions in D_2O	Energy scale, detector response
pT	γ	19.8	multiple positions in D_2O	Energy scale, detector response
^{252}Cf	neutron	$(0, 6)$	multiple positions in D_2O	n detection efficiency
^{241}Am^{9}Be	neutron	(0–9)	multiple positions in D_2O	n detection efficiency
^{24}Na	β, γ	< 1.4 (β), 2.7 (γ)	uniform in D_2	n detection efficiency
^{222}Rn	β, γ	(0–3.2)	uniform in D_2 and H_2O	Background studies
laser-ball	light		multiple positions in D_2O	PMT eq. + D_2O, H_2O optics

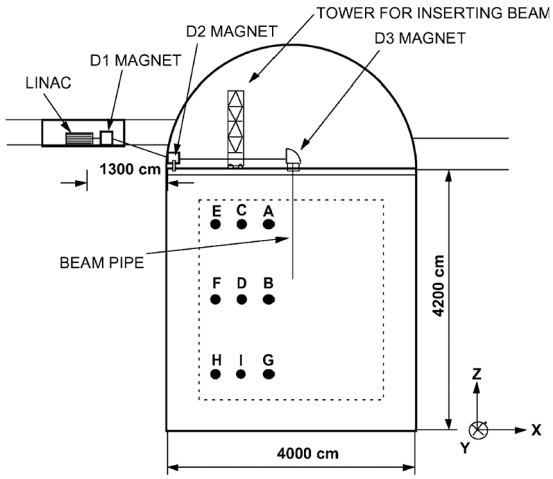

Fig. 3. Super-Kamiokande: scheme of the Linac system.

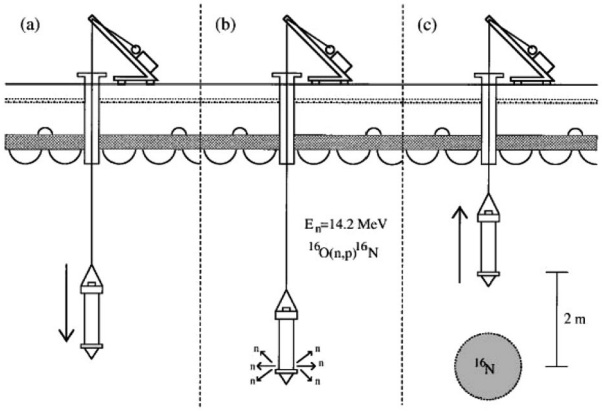

Fig. 4. Super-Kamiokande: overview of the ^{16}N deployment. (a) the DTG is lowered in the detector at the desired position; (b) it is fired; (c) it is withdrawn 2 meters and data are collected.

Water transparency measurement

Given the large size of Super-Kamiokande, the detector response is crucially dependent on light propagation effects which must therefore be studied carefully and monitored in time (see [18]). A direct measurement of light attenuation of the Super-Kamiokande water is performed with a diffuser-ball illuminated by a titanium-sapphire laser through an optical fiber. The diffuser is deployed (on the vertical axis) at different depths in water and is imaged by a CCD camera. This operation is performed periodically for different wavelenghts. The typical attenuation lenght for $\lambda = 420$ nm is measured to be ~ 100 m. Light attenuation in water is a combined effect of absorption and scattering. In order to disentangle the two contributions an other system is used. In this case, the light provided by dye and N_2 lasers at different wavelenghts (337, 371, 400 and 420 nm) is shot at the top of the detector pointing downwards and is detected by the Super-Kamiokande photomultipliers: the analysis is then performed under the assumption that PMT hits clustered at the bottom of the tank are due to unscattered photons, while the remaining hits, in barrel and top PMTs, are due to photons scattered in the water and/or reflected by the bottom PMTs. The light attenuation length in water is also measured by using through-going cosmic ray muons.

3.3 Calibrations in Borexino

Borexino detects solar neutrinos via the reaction

$$\nu_x + e^- \rightarrow \nu_x + e^-$$

on electrons of 300 tons of liquid scintillator. The main goal of the experiment is to study the low energy portion of the solar neutrino spectrum, which is unaccessible to water Cherenkov detectors, like SNO and Super-Kamiokande. Since scintillator light doesn't provide directional information, the neutrino signal is virtually indistinguishable from radioactive background and therefore the key requirement for the success of the experiment is radiopurity. Calibrations must take this into account and all the components of the calibration system must comply with strict radiopurity constraints. Borexino analysis demands a complete knowledge of the detector response: the energy scale must be known with high precision and in a large energy range (between 0.1 and 10 MeV), since the

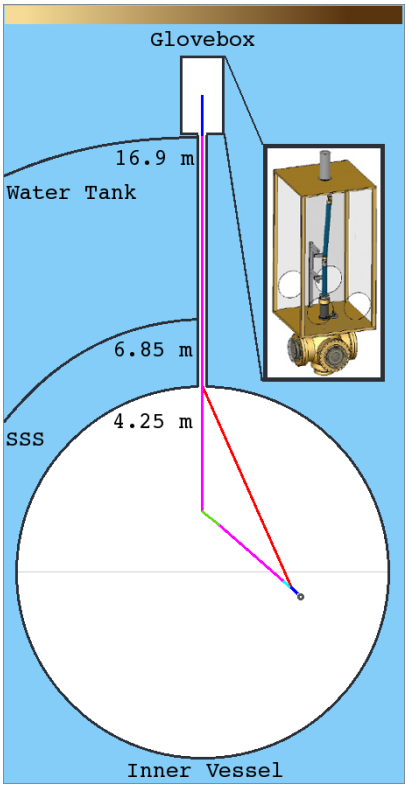

Fig. 5. Borexino: schematic view of the internal source deployment system.

different solar neutrino fluxes are extracted from a fit to the scattered electron energy spectrum. Moreover, given the large dimensions of the detector, the energy response must be mapped carefully throughout the scintillator volume. Finally, since the analysis rely on mass fiducialization, it is important to reduce the systematic error associated to position reconstruction which impacts directly on the neutrino flux measurements through the evaluation of the target mass.

Borexino has performed several calibration campaigns which involved the insertion of sources in the scintillator volume (internal calibrations) or in the buffer region (external calibrations).

Internal calibrations

The internal calibration system of the Borexino detector is shown in fig. 5. It consists of a series of interconnecting hollow rods, that can be assembled together and deployed in the scintillator volume. A flexible Teflon tether tube enters the detector with the rods and is fixed at the end of the last rod where also the source is hold; the tether is used to adjust the hinge angle to the desired position. It is also a crucial part of the source location system since it conveys light from an external laser to a diffuser ball mounted close to the source itself. Seven digital cameras mounted on the Stainless Steel Sphere (where also the phototubes are mounted) take a picture while the diffuser ball is flashed thus providing the source position with an accuracy of approximately 1 cm.

All components entering the detector have to meet strict cleanliness requirements in order to preserve the excellent scintillator radiopurity. Any operations on the deployment system is performed through a glovebox installed in a Class 100 clean-room atop the detector.

Since the beginning of data-taking, Borexino has performed four internal calibration campaigns between October 2008 and July 2009. During these campaigns, sources of different types (α, β, γ and neutrons) and energies were deployed in about three hundred different locations throughout the scintillator volume. Most of the sources were prepared by dissolving the radioactive isotope in a small volume of liquid (about 6 ml) and sealing it in 1 inch diameter quartz vials.

The vast majority of calibration points was collected with a ^{14}C-^{222}Rn source which provides α, β and γ's in the energy range of interest for Borexino, between 0 and 3.2 MeV. These data were used to study the position reconstruction performance and to check the uniformity of the detector response throughout the scintillator volume. Thanks to this analysis, the systematic error due to the Fiducial Volume has been reduced to $\sim 1\%$.

Several mono-energetic γ sources have been deployed to study the absolute energy scale between 0.122 MeV (^{57}Co) and 1.46 MeV (^{40}K). The activity of the sources was around 2 Bq. In one case (^{85}Sr, $E_\gamma = 514$ keV) the source was deployed in several points on the border of the fiducial volume and was used as a reference point for detection efficiency studies.

In order to have calibration points at energies up to about 10 MeV a ^{241}Am^{9}Be source was used. AmBe provides neutrons and also γ's with energy up to $\sim$ 9 MeV from neutron capture on protons or other nuclei in the source holder.

Details on the sources type, energies and deployment positions are given in table 2.

Figure 6 shows an example of the Borexino calibration results: the energy specta obtained with the γ sources deployed in the scintillator during one of the calibration campaigns. The sources are ^{57}Co, ^{139}Ce, ^{203}Hg, ^{85}Sr, ^{54}Mn, ^{65}Zn, ^{40}K, and ^{60}Co. These data were essential to fine-tune the Monte Carlo code in reproducing the scintillator non-linear energy response. The agreement between data (black curves) and Monte Carlo (blu curves) is within 0.2%.

A dedicated analysis showed that the Borexino calibration system worked properly without leaving any detectable radioactivity in the scintillator. More details on the Borexino internal calibration system can be found in [17].

External calibrations

In addition to the internal calibration system, Borexino has developed the so-called external calibration system which allows to deploy calibration sources in the outer buffer region, close to the Stainless Steel Sphere surface where the Borexino PMTs are mounted. This system consists in fourteen re-entrant tubes mounted on the SSS and

Table 2. Borexino: summary of the internal calibration sources.

Source	Type	E [MeV]	Position
^{57}Co	γ	0.122	in IV volume
^{139}Ce	γ	0.165	in IV volume
^{203}Hg	γ	0.279	in IV volume
^{85}Sr	γ	0.514	z-axis + sphere $R = 3$ m
^{54}Mn	γ	0.834	along z-axis
^{65}Zn	γ	1.115	along z-axis
^{60}Co	γ	1.173, 1.332	along z-axis
^{40}K	γ	1.460	along z-axis
^{222}Rn + ^{14}C	β, γ	0–3.20	in IV volume
	α	5.5, 6.0, 7.4	in IV volume
^{241}Am^{9}Be	n, γ	0–9	sphere $R = 4$ m
394 nm laser	light	–	center

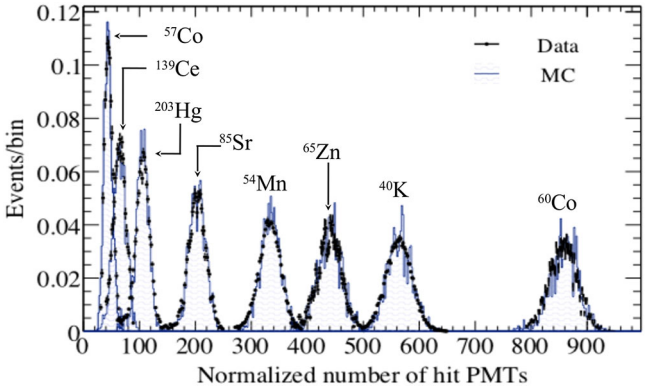

Fig. 6. Borexino: energy spectra of γ lines from eight different calibration sources expressed in terms of the normalized number of hit PMTs.

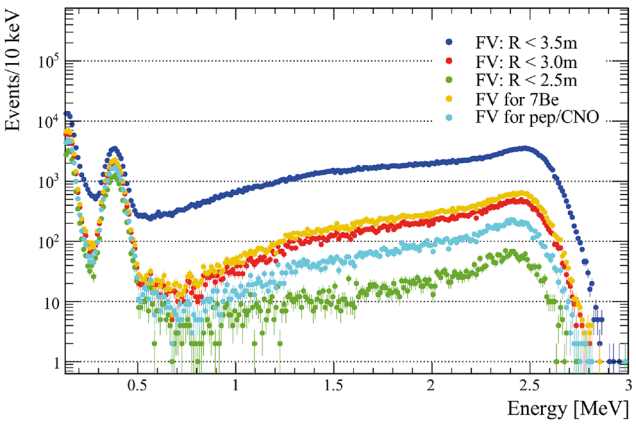

Fig. 7. Borexino external calibrations: the energy spectra of external γ-rays emitted by the 228 Th source. Different colours correspond to different Fiducial Volume selections.

connected to the outside top detector platform via flexible polyethylene tubes. During two calibration campaigns (2010–2011), a custom-made ^{228}Th source was inserted in different tubes to study the spectral shape and radial dependence of external background (typically 2.6 MeV gammas from the ^{208}Tl decay). Moreover, the Borexino external calibration helped in studying disuniformities in the detector energy response for events far from the center and in precisely determining the inner vessel shape.

Figure 7 shows the energy spectra of external γ-rays emitted by the ^{228}Th source. Different colours correspond to different Fiducial Volume selections. More details on the Borexino external calibration system can be found in [17].

Trigger efficiency

Borexino was able to make a complete spectroscopy of solar neutrinos, including the lowest energy ones, the pp neutrinos. A test of the trigger efficiency down to low energies was made with laser light exploiting the PMT equalization system [16]. This study showed that the trigger efficiency is $> 99.999\%$ for energies greater than 120 keV. An independent study of the trigger efficiency was performed at higher energies ($E = 514$ keV) using a ^{85}Sr source with known activity placed in different points of the detector volume (see table 2). The efficiency was found to be consistent with unity in all positions [17].

3.4 Calibrations in KamLAND

The Kamioka Liquid scintillator Anti-Neutrino Detector (KamLAND) consists of 1 kton of liquid scintillator. The main goal of the experiment is to study neutrino oscillations by detecting reactor anti-neutrinos with a baseline of ~ 200 km. Starting from 2009, after an intensive purification campaign, KamLAND improved its liquid scintillator

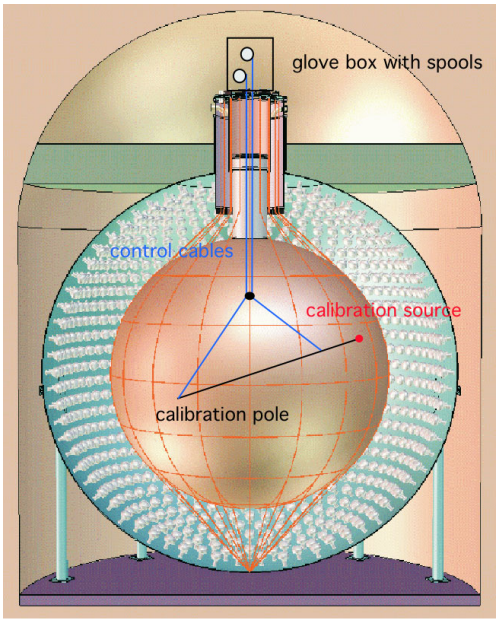

Fig. 8. KamLAND: scheme of the off-axis calibration system.

radiopurity making it possible to also study solar neutrinos via the elastic scattering reaction

$$\nu_x + e^- \rightarrow \nu_x + e^-.$$

Calibrations have been routinely performed in KamLAND, by lowering several radioactive or optical sources into the scintillator volume. The KamLAND calibration system has to meet severe safety requirements to preserve the thin nylon vessel integrity, must be built with materials compatible with the aggressive liquid scintillator and must exhibit precise and reproducible positioning of the sources. The standard calibration system employed since 2005 in KamLAND is described in [21]. It is designed to reach nearly all positions throughout the detector volume by means of a segmented pole manipulated by two control cables. The source is attached to one extremity and is positioned throughout the fiducial volume by adjusting the pole orientation and lenght (see fig. 8). Motion control and cable spool system are located inside a glovebox on top of the detector.

This system was crucial to reduce the uncertainty in the fiducial volume by more than a factor two and allowed to study systematic biases in vertex and energy reconstruction for the anti-neutrino reactor analysis. However, it was not designed to comply with the much stricter radiopurity requirements of the solar neutrino data-taking phase. For this reason, after the beginning of the high-purity phase a new, ultra-clean, source deployment system has been realized, called MiniCal (see [22]). This system is able of deploying sources only on the z-axis by means of a stepper motor which turns a spool of cable. The cable is chosen to be thin (compared with previously used cables) to make the system more compact and to reduce the amount of materials in contact with the scintillator. In order to prevent radon intrusion, the MiniCal hardware is enclosed within an hermetically sealed housing. The motion of the cable is measured by an encoded pulley located above the z-axis, which enables positioning of the source with a precision of 2 mm. The system was used starting from 2009 to deploy several gamma sources covering the energy range of interest for solar neutrinos: ^{7}Be, ^{60}Co, ^{68}Ge, ^{85}Sr, ^{137}Cs, and ^{203}Hg. The absolute energy scale, including the effects of scintillator quenching and Cherenkov light production is determined from this set of calibration data and is an essential element in the solar neutrino analysis performed by KamLAND [23].

4 Conclusions

In this article we have reviewed the calibration strategies adopted by the radiochemical (Homestake, Gallex, SAGE) and the real-time (Kamiokande, Super-Kamiokande, SNO, KamLAND, Borexino) solar neutrino experiments. In particular, we have shown that calibrations have been essential for the success of solar neutrino experiments.

References

1. C.M. Cattadori, L. Pandola, *Experimental and analysis methods in radiochemical experiments*, contribution to this Topical Issue.
2. Y. Koshio, *Data analysis in solar neutrinos by water Cherenkov detectors*, contribution to this Topical Issue.
3. G. Testera, *Data analysis in solar neutrino liquid scintillator detectors*, contribution to this Topical Issue.
4. A.M. Serenelli, *Alive and well: A short review about standard solar models*, contribution to this Topical Issue.
5. M. Maltoni, A.Y. Smirnov, *Solar neutrinos and neutrino physics*, contribution to this Topical Issue.
6. B. Cleveland *et al.*, Astrophys. J. **496**, 505 (1998).
7. W. Hampel *et al.*, Phys. Lett. B **420**, 114 (1998).
8. W. Hampel *et al.*, Phys. Lett. B **436**, 158 (1998).
9. J.N. Abdurashitov *et al.*, Phys. Rev. C **59**, 2246 (1999).
10. J.N. Abdurashitov *et al.*, Phys. Rev. C **73**, 045805 (2006).
11. M.R. Dragowsky *et al.*, Nucl. Instrum. Methods A **481**, 284 (2002).
12. N.J. Tagg *et al.*, Nucl. Instrum. Methods A **489**, 178 (2002).
13. A.W.P. Poon *et al.*, Nucl. Instrum. Methods A **452**, 115 (2000).
14. K. Boudjemline *et al.*, Nucl. Instrum. Methods A **620**, 171 (2010).
15. B.A. Moffat *et al.*, Nucl. Instrum. Methods A **554**, 255 (2005).
16. H. Back *et al.*, J. Instrum. **7**, 10018 (2012).
17. B. Caccianiga *et al.*, Nucl. Instrum. Methods A **496**, 353 (2003).
18. S. Fukuda *et al.*, Nucl. Instrum. Methods A **501**, 418 (2003).
19. M. Nakahata *et al.*, Nucl. Instrum. Methods A **421**, 113 (1999).
20. E. Blaufuss *et al.*, Nucl. Instrum. Methods A **458**, 636 (2001).
21. B.E. Berger *et al.*, J. Instrum. **4**, 04017 (2009).
22. T.I. Banks *et al.*, Nucl. Instrum. Methods A **769**, 88 (2015).
23. A. Gando *et al.*, arXiv:1405.6190v1 (2014).